

Nonequilibrium Tuning of the Thermal Casimir Effect

David S. Dean,¹ Bing-Sui Lu,² A. C. Maggs,³ and Rudolf Podgornik²

¹*Univ. Bordeaux and CNRS, Laboratoire Ondes et Matière d'Aquitaine (LOMA), UMR 5798, F-33400 Talence, France*

²*Department of Theoretical Physics, J. Stefan Institute and Department of Physics, Faculty of Mathematics and Physics, University of Ljubljana, SI-1000 Ljubljana, Slovenia*

³*UMR Gulliver 7083 CNRS, ESPCI ParisTech, PSL Research University, 10 rue Vauquelin, 75005 Paris, France*

(Received 21 April 2016; published 14 June 2016)

In net-neutral systems correlations between charge fluctuations generate strong attractive thermal Casimir forces and engineering these forces to optimize nanodevice performance is an important challenge. We show how the normal and lateral thermal Casimir forces between two plates containing Brownian charges can be modulated by decorrelating the system through the application of an electric field, which generates a nonequilibrium steady state with a constant current in one or both plates, reducing the ensuing fluctuation-generated normal force while at the same time generating a lateral drag force. This hypothesis is confirmed by detailed numerical simulations as well as an analytical approach based on stochastic density functional theory.

DOI: [10.1103/PhysRevLett.116.240602](https://doi.org/10.1103/PhysRevLett.116.240602)

Electromagnetic (EM) fluctuation-induced interactions are dominant in micro-electro-mechanical systems (MEMS) [1], and their presence is often viewed as undesirable as they engender stiction between the micron-sized components of the MEMS devices. Controlling, or engineering, these forces is, however, difficult as although they are all of electromagnetic origin, they have contributions from both thermal and quantum fluctuations as well as from different microscopic charge multipoles, e.g., ubiquitous dipoles [2] and sometimes also free monopoles [3].

Lifshitz [4] reformulated and generalized the original zero-point electromagnetic field theory of idealized conducting plates, proposed by Casimir [2,5–7], in terms of the dielectric and magnetic permeabilities of real materials sampled at all Matsubara frequencies including a thermal zero frequency contribution. The Lifshitz formula for EM field fluctuation-induced forces in symmetric interaction configurations between standard materials reveals this interaction is generically attractive [8]. Since the interaction depends on frequency dependent material response properties, it also suggests an immediate means of modulating or even designing the Casimir force by appropriate changes in the material's properties. While this line of reasoning has been followed successfully in metamaterials, it may be more useful to have a means of switching EM fluctuation induced interactions directly *in situ*. A switchlike induced change in the optical properties of a material indeed yields experimentally measurable differences in the interaction between bodies in a number of cases, e.g., light or laser sources can modify the charge carrier densities in semiconductors [9,10], or induce phase changes [11]. Theoretically, it has been shown that the quantum Hall effect modified conductivity can also be used to modify Casimir forces between graphene sheets [12]. Holding

interacting materials at different temperatures also allows modifications of Casimir interactions [13–21].

An alternative to the Lifshitz field-based formulation is presented by the Schwinger matter-based approach where the Casimir force originates in interactions between fluctuating charges and currents [6,22,23]. Within this conceptual framework the attraction between materials can be understood as being due to correlations between microscopic EM source charge fluctuations that in general reduce their (free) energy. This implies that the effect of nonequilibrium driving the sources with an external electric or magnetic field will *scramble* the system's ability to develop charge correlations and could thus in general reduce the attraction between the materials. The scenario of engineering the EM fluctuation interactions by applying external driving fields to MEMS is relatively easily implemented compared to the switching mechanisms based on material properties modifications discussed above, and thus may be a promising technological direction worth pursuing in detail.

In order to test the nonequilibrium driving hypothesis and assess its ramifications, we analyze the system of two parallel conducting plates, where only one of them is subjected to a current-inducing applied external electric field in a closed circuit configuration. For systems with currents the usual methods of equilibrium statistical mechanics do not apply. We propose a methodology to study the effect of an imposed current in the nonequilibrium steady state configuration on both the normal and lateral forces. The response of these forces to driving is surprisingly rich and this study thus opens up new perspectives for direct *in situ* control of the EM fluctuation interactions.

We analyze a well-defined classical 2D jellium model, which can be studied out of equilibrium both numerically and analytically, composed of two parallel plates with

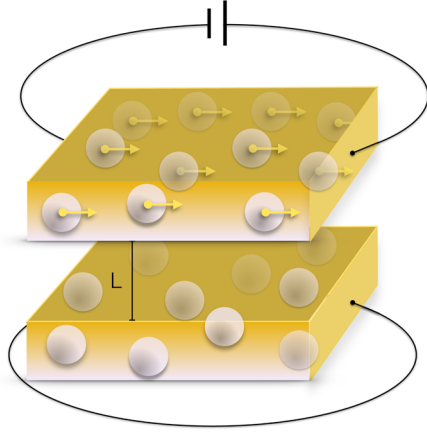


FIG. 1. Schematic depiction of plates (1 and 2) containing mobile charges, with an external electric field \mathbf{E}_{01} applied to plate 1 in a closed circuit configuration, driving a current flow in the plate setup using a battery. The circuit of both plates [27] is open so charge flows through the system rather than accumulating at the edges of the plates.

mobile charged Brownian particles embedded within a uniform background charge sheet [24–26]; see Fig. 1. In equilibrium, at high temperatures in the weak coupling limit, the two plates exhibit the universal thermal Casimir force $F_{\perp} = -[TS\zeta(3)/8\pi L^3]$ at large interplate separations L , with S denoting the area of the plates, ζ the Riemann zeta function, and T the temperature of the two plates, assumed to be the same for both. To explore the effect of an electric field on one of the plates we need to specify the dynamics of the charges and we adopt a Langevin model [21,28], where a charge in the plate α at the point \mathbf{X} obeys the overdamped Langevin equation

$$\frac{d\mathbf{X}}{dt} = \beta D_{\alpha} q_{\alpha} \mathbf{E}_{\parallel\alpha}(\mathbf{X}) + \sqrt{2D_{\alpha}} \boldsymbol{\eta}_{\alpha}, \quad (1)$$

where $\boldsymbol{\eta}_{\alpha}$ is a zero-mean Gaussian white noise with correlation function $\langle \eta_{\alpha i}(t) \eta_{\alpha j}(t') \rangle = \delta_{\alpha\alpha'} \delta_{ij} \delta(t-t')$ and $\mathbf{E}_{\parallel\alpha}(\mathbf{X})$ is the local in-plane electric field in the plate α , generated by the electric charge distributions in both plates as well as any externally applied electric field. In addition, D_{α} denotes the diffusion constant of the charges and β [29] the inverse temperature so that βD_{α} is the local mobility, as deduced from the Einstein relation. Finally, q_{α} is the charge of the mobile Brownian particles in the plate α and if \bar{n}_{α} denotes the average density of charge carriers in plate α ; the uniform neutralizing surface charge density is thus $\sigma_{\alpha} = -\bar{n}_{\alpha} q_{\alpha}$. The idealized model above is amenable to both detailed numerical as well as analytical developments, confirming our basic hypothesis that the driving field modifies the charge correlation between the plates, thus leading to a modified thermal Casimir force in direction normal as well as lateral to the plates.

Numerical simulations.—The two-plate system was simulated by integrating the Langevin equations (1) for

Brownian particles [30]; the electrostatic forces due to the charges are computed via Ewald summation. We use a noncubic box of dimensions $H \times H \times 3H$, with periodic boundary conditions in each direction. We studied several separations between the plates up to a maximum distance of $L = 0.12H$; beyond this distance the interaction between plates can be shown to cross over to an exponential form due to the discrete Fourier modes within the simulation box. In this noncubic geometry the undesired interactions between images of plates in the z direction are known to be negligible [35]. We worked with a variable total number of particles, $N = 1000$, $N = 2000$, $N = 4000$ in order to control finite size errors in the simulation. Apart from the applied electric field \mathbf{E}_{01} , causing a current to flow within plate 1, the two plates are identical (the charges are identical and of the same number $N/2$ in each plate, the diffusion constants and temperatures are also the same). Plate separations are taken such that we find the far field universal Casimir effect at zero applied field.

The normal and lateral force acting on the plate α are computed from the formulas

$$\mathbf{F}_{\perp, \parallel\alpha}(L) = q_{\alpha} \int_{S_{\alpha}} d^2\mathbf{x} \mathbf{E}_{\perp, \parallel\alpha}(\mathbf{x}) \Delta n_{\alpha}(\mathbf{x}), \quad (2)$$

where $n_{\alpha}(\mathbf{x}) = \sum_i \delta(\mathbf{X}_i - \mathbf{x})$ is the density of mobile charge carriers and $\Delta n_{\alpha}(\mathbf{x}) = n_{\alpha}(\mathbf{x}) - \bar{n}_{\alpha}$ is the fluctuation about its spatially averaged value \bar{n}_{α} , which is the same as that of the neutralizing uniform background charge. In Eq. (2) \perp, \parallel indicate the direction with respect to the bounding plates. The electrostatic potential $\phi(\mathbf{x})$ in plate α has contributions both from plate α as well as plate α' (opposite) mediated by the standard Coulomb interaction, while the dielectric constant ϵ is assumed to be homogeneous.

The numerical results for the average of the two forces are plotted in Fig. 2. They are both fluctuational in nature, and, in principle, the statistics of the force can be measured. For small driving fields the normal Casimir force saturates to the equilibrium thermal Casimir force, while the lateral force vanishes in equilibrium. As the field increases there is a *monotonic* decrease in the amplitude of the normal force, that eventually asymptotes to zero, and a *nonmonotonic* variation of the lateral force that is zero for small as well as large values of the driving field.

Dynamical density functional theory.—The density fields $n_{\alpha}(\mathbf{x}, t)$ in each plate evolve according to the exact stochastic partial differential equation [36,37]

$$\begin{aligned} \frac{\partial n_{\alpha}(\mathbf{x}, t)}{\partial t} = & D_{\alpha} \nabla_{\parallel} \cdot [\nabla_{\parallel} n_{\alpha}(\mathbf{x}, t) - \beta_{\alpha} q_{\alpha} \mathbf{E}_{\parallel\alpha} n_{\alpha}(\mathbf{x}, t)] \\ & + \nabla_{\parallel} \cdot [\sqrt{2D_{\alpha} n_{\alpha}(\mathbf{x}, t)} \boldsymbol{\eta}_{\alpha}(\mathbf{x}, t)]. \end{aligned} \quad (3)$$

In this density representation of the dynamics, the noise $\boldsymbol{\eta}_{\alpha}(\mathbf{x}, t)$ is a spatiotemporal Gaussian white noise vector

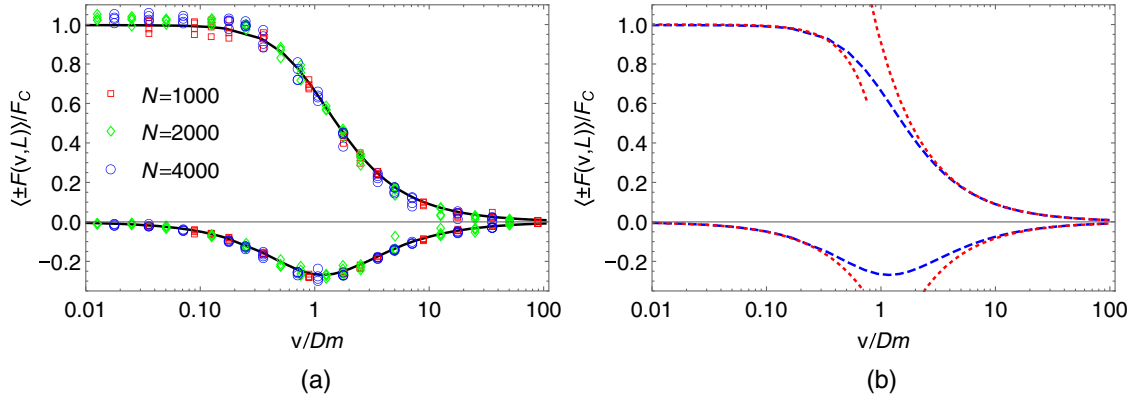


FIG. 2. (a) Evolution of the amplitude of the perpendicular and transverse components of the Casimir force with the driving field, normalized by the thermal Casimir force, $F_C = -TS\zeta(3)/8\pi L^3$. For ease of comparison, we have displayed the component of the normalized tangential force that is parallel to the driving field, with a sign opposite to that of the normalized perpendicular force. Simulation results are taken from systems with $N = 1000$ (red squares), $N = 2000$ (green diamonds), and $N = 4000$ (blue circles). For each value of N the interaction is evaluated for four separations: $L = 0.02H$, $L = 0.05H$, $L = 0.08H$, $L = 0.12H$. The vertical data spread corresponds to residual systematic, finite size errors in the simulations. The theoretical predictions, Eqs. (9), (10) for $L \times m = 2000$ are shown by black solid curves. (b) Evolution of the amplitude of the perpendicular and transverse components of the Casimir force between identical plates ($D_1 = D_2 = D$, $m_1 = m_2 = m$) with the driving field, normalized by the universal thermal Casimir force. Theoretical predictions, Eqs. (9), (10) for $Lm = 2000$ are shown by blue dashed curves, while the corresponding small field and large field asymptotes, Eqs. (11), (12), (13), (14), are shown as the red, dotted curves.

field of mean zero and with correlation function $\langle \eta_{ai}(\mathbf{x}, t) \eta_{a'j}(\mathbf{x}', t) \rangle = \delta_{aa'} \delta_{ij} \delta(t - t') \delta(\mathbf{x} - \mathbf{x}')$.

To make analytical progress we expand the deterministic term in Eq. (3) to linear order in the density fluctuations n_α and the noise term to zeroth order (since it is of zero mean this is consistent with the first order expansion of the deterministic terms). This approximation has already been used to examine interactions between plates out of equilibrium in, e.g., evolution to the equilibrium force for initially out-of-equilibrium plates [28], as well as for the nonequilibrium force between plates held at different temperatures [21]. This small density expansion was recently shown to reproduce Onsager's classical results on the conductivity of strong electrolyte solutions [38] in a very straightforward and compact manner [39]. Within the small density fluctuation approximation the two dimensional Fourier transform of the density fluctuations, defined as $\Delta \tilde{n}_\alpha(\mathbf{Q}, t) = \int_{S_\alpha} d^2 \mathbf{x} \exp(-i\mathbf{Q} \cdot \mathbf{x}) \Delta n_\alpha(\mathbf{x}, t)$, has a steady state correlation function $\langle \Delta \tilde{n}_\alpha(\mathbf{Q}) \Delta \tilde{n}_{\alpha'}(\mathbf{Q}') \rangle = (2\pi)^2 \delta(\mathbf{Q} + \mathbf{Q}') C_{\alpha\alpha'}(\mathbf{Q})$, which obeys [40]

$$M_{\alpha\gamma}(\mathbf{Q}) C_{\gamma\alpha'}(\mathbf{Q}) + C_{\alpha\gamma}(\mathbf{Q}) M_{\gamma\alpha'}^\top(-\mathbf{Q}) = 2\delta_{\alpha\alpha'} D_\alpha \bar{n}_\alpha Q^2. \quad (4)$$

The matrix $M(\mathbf{Q})$ is given by

$$M_{\alpha\gamma}(\mathbf{Q}) = Q^2 (\tilde{D}_\alpha \delta_{\alpha\gamma} + \beta q_\alpha q_\gamma \bar{n}_\gamma D_\alpha \tilde{G}(\mathbf{Q}, z_{\alpha\gamma})), \quad (5)$$

where $\tilde{D}_\alpha = D_\alpha (1 - i\beta q_\alpha \bar{n}_\alpha \hat{\mathbf{Q}} \cdot \mathbf{E}_{0\alpha}/Q)$, $z_{\alpha\gamma} = z_\alpha - z_\gamma$, and $\hat{\mathbf{Q}}$ is the unit wave vector. The term $\tilde{G}(\mathbf{Q}, z_{\alpha\gamma})$ denotes

the in-plane Fourier transform of the Coulomb interaction $G(\mathbf{x}, z)$ (without the charge factors) and is given by $\tilde{G}(\mathbf{Q}, z) = \exp(-Q|z|)/2\epsilon Q$. The components of the fluctuation force in Eq. (2) can be expressed as

$$\langle F_\perp \rangle = -q_1 q_2 \int_{S_1} d\mathbf{x} \int_{S_2} d\mathbf{y} \langle \Delta n_1(\mathbf{x}) \Delta n_2(\mathbf{y}) \rangle \frac{\partial G(\mathbf{x} - \mathbf{y}, L)}{\partial L} \quad (6)$$

and

$$\langle \mathbf{F}_\parallel \rangle = -q_1 q_2 \int_{S_1} d\mathbf{x} \int_{S_2} d\mathbf{y} \langle \Delta n_1(\mathbf{x}) \Delta n_2(\mathbf{y}) \rangle \nabla_\parallel G(\mathbf{x} - \mathbf{y}, L). \quad (7)$$

The Fourier transform of $\langle \Delta n_\alpha(\mathbf{x}) \Delta n_\beta(\mathbf{y}) \rangle$ can then be obtained from Eq. (4), which together with the definitions Eqs. (6), (7) yield the average normal and lateral force. Defining,

$$f(Q, L) = \log \left(1 + \Delta(\mathbf{v}_1, \mathbf{v}_2)^2 - \frac{m_1 m_2 \exp^{-2QL}}{(m_1 + 2Q)(m_2 + 2Q)} \right), \quad (8)$$

with $\mathbf{v}_\alpha = \beta q_\alpha D_\alpha \mathbf{E}_{0\alpha}$ the average velocity of the mobile charges in the plate α , $m_\alpha = \beta \bar{n}_\alpha q_\alpha^2 / \epsilon$ is the inverse screening length for a 2D Coulomb gas of mobile charges in equilibrium, and $\Delta(\mathbf{v}_1, \mathbf{v}_2) = 2[\hat{\mathbf{Q}} \cdot (\mathbf{v}_1 - \mathbf{v}_2)] / [D_1 m_1 + D_2 m_2 + 2(D_1 + D_2)Q]$, we can write [30]

$$\langle F_{\perp}(L) \rangle = -\frac{1}{2}TS \int \frac{d^2\mathbf{Q}}{(2\pi)^2} \frac{\partial f(Q, L)}{\partial L}, \quad (9)$$

and

$$\langle \mathbf{F}_{\parallel}(L) \rangle = TS \int \frac{d^2\mathbf{Q}}{(2\pi)^2} \frac{\partial f(Q, L)}{\partial L} \hat{\mathbf{Q}} \Delta(\mathbf{v}_1, \mathbf{v}_2). \quad (10)$$

We note that when $\mathbf{v}_1 - \mathbf{v}_2 = 0$ we recover the expression for the equilibrium thermal Casimir force for $\langle F_{\perp}(L) \rangle$, while the lateral force is zero, since in the common rest frame of the moving charges the system is in equilibrium.

The normal force is monotonic in its variation with respect to the relative difference of the bare velocity of the charges in each plate. In the far field limit, where $L \gg m_1^{-1}$, m_2^{-1} and when, in addition, $|\mathbf{v}_1 - \mathbf{v}_2| \ll u_1, u_2$, where $u_{\alpha} = D_{\alpha} m_{\alpha}$ define an intrinsic velocity scale in each plate, the average force simplifies to give

$$\langle F_{\perp}(L) \rangle \approx -\frac{TS}{8\pi L^3} \left[\zeta(3) - \frac{\pi^2 |\mathbf{v}_1 - \mathbf{v}_2|^2}{3(u_1 + u_2)^2} \right]. \quad (11)$$

The effect of the applied field can thus be seen as renormalizing the effective *Hamaker* constant associated with the $1/L^3$ power law. The far field fluctuation induced attraction between the plates thus monotonically decreases upon increasing the relative velocity. In the opposite limit of large relative velocity, we find that the force decays as

$$\langle F_{\perp}(L) \rangle \approx -\frac{TS}{32\pi L^3} \frac{(u_1 + u_2)}{|\mathbf{v}_1 - \mathbf{v}_2|} \left[8 - \frac{\pi^2}{3} - 8 \ln 2 + 4 \ln^2 2 \right]. \quad (12)$$

Contrary to the normal force, the lateral force is not monotonic in the relative velocity and shows a well-defined maximum. On the two sides of this minimum the lateral force behaves as

$$\langle F_{\parallel}(L) \rangle \approx -\frac{TS}{16\pi L^3} \frac{(u_1 + u_2)}{|\mathbf{v}_1 - \mathbf{v}_2|} \quad (13)$$

in the large field limit, and for small fields as

$$\langle F_{\parallel}(L) \rangle \approx -\frac{TS |\mathbf{v}_1 - \mathbf{v}_2|}{8\pi L^3 (u_1 + u_2)} \left[\zeta(3) - \frac{\pi^2 |\mathbf{v}_1 - \mathbf{v}_2|^2}{128(u_1 + u_2)^2} \right]. \quad (14)$$

A similar nonmonotonic drag force has recently been predicted for single particles coupled to thermally fluctuating classical fields [41,42].

In Fig. 2(a) we compare the theoretical predictions, Eqs. (9), (10), for the normal and lateral forces with the results of our numerical simulations. We see that, despite the relatively low temperature of the system, the agreement

for both forces is excellent. The asymptotic results for the small and large field limits, Eqs. (11), (12), (13), (14), are compared to the full numerical integration of Eqs. (9), (10) in Fig. 2(b).

Conclusions.—We have introduced a simple model exhibiting the thermal Casimir effect and shown that when the system is driven by an external electric field, the thermal Casimir force, both its normal and lateral components can be modulated in a controlled and reversible manner. The underlying physical mechanism is that the external driving electric fields suppress the charge correlations that are responsible for the fluctuation interaction. Indeed, the Onsager study of the field dependence of electrolyte conductivity [38], the Wien effect, shows that the increase in conductivity is due to the fact that the applied field suppresses Debye screening. The underlying mechanism here is clearly related and we have clearly exhibited the effect in numerical simulations, and, analytically, taking into account all the nonequilibrium physics in the model via its microscopic formulation. Indeed, one of the prime advantages of the model studied here is that one can carry out numerical experiments to measure fluctuation induced interactions *out of equilibrium* and future study of this model should enable the study of fluctuation induced interactions beyond the weak density fluctuation approximation employed in our analytical study.

Extensions of this model to more realistic systems or models are clearly desirable in order to test the general hypothesis on field-induced correlation scrambling put forward here. Another natural question to ask is whether nonequilibrium forcing can be used to amplify correlations and thus enhance the fluctuation-induced attractive force? The Brownian conductor model should be extended to take into account inertial effects so that it more closely resembles the Drude model. In addition, retardation effects in the electromagnetic interactions between the charges could also be incorporated. Ultimately, one should consider nonequilibrium quantum field theories in order to understand the quantum aspects of the problem. Clearly ac driving fields also constitute an interesting line of research, from both a numerical and analytical point of view.

This work was partially financed by a Joliot Chair of the ESPCI (RP), the ANR FISICS (DSD), and the ANR FSCF (ACM) and ARRS P1-0055 (BSL).

-
- [1] P. Ball, *Nature (London)* **447**, 772 (2007).
 - [2] V. M. Mostepanenko and N. N. Trunov, *The Casimir Effect and Its Applications* (Clarendon Press, Oxford, 1997).
 - [3] D. Drosdoff, I. V. Bondarev, A. Widom, R. Podgornik, and L. M. Woods, *Phys. Rev. X* **6**, 011004 (2016).
 - [4] E. M. Lifshitz, *Sov. Phys. JETP* **2**, 73 (1956).
 - [5] H. B. G. Casimir, *Proc. Koninklijke Nederlandse Akad. Wetenschappen B* **51**, 793 (1948).

- [6] K A Milton, *The Casimir Effect, Physical Manifestations of Zero-Point Energy* (World Scientific, Singapore, 2001).
- [7] D. Dalvit, P. Milonni, D. Roberts, and F. Rosa, *Casimir Physics*, Lecture Notes in Physics (Springer-Verlag, Berlin, Heidelberg, 2011), Vol. 834.
- [8] V. A. Parsegian, *Van der Waals Forces* (Cambridge University Press, Cambridge, England, 2006).
- [9] W. Arnold, S. Hunklinger, and K. Dransfeld, *Phys. Rev. B* **19**, 6049 (1979).
- [10] F. Chen, G. L. Klimchitskaya, V. M. Mostepanenko, and U. Mohideen, *Phys. Rev. B* **76**, 035338 (2007).
- [11] G. Torricelli, P. J. van Zwol, O. Shpak, C. Binns, G. Palasantzas, B. J. Kooi, V. B. Svetovoy, and M. Wuttig, *Phys. Rev. A* **82**, 010101 (2010).
- [12] W.-K. Tse and A. H. MacDonald, *Phys. Rev. Lett.* **109**, 236806 (2012).
- [13] I. A. Dorofeyev, *J. Phys. A* **31**, 4369 (1998).
- [14] M. Antezza, L. P. Pitaevskii, and S. Stringari, *Phys. Rev. Lett.* **95**, 113202 (2005).
- [15] M. Antezza, L. P. Pitaevskii, S. Stringari, and V. B. Svetovoy, *Phys. Rev. A* **77**, 022901 (2008).
- [16] G. Bimonte, *Phys. Rev. A* **80**, 042102 (2009).
- [17] M. Krüger, T. Emig, G. Bimonte, and M. Kardar, *Europhys. Lett.* **95**, 21002 (2011).
- [18] M. Krüger, T. Emig, and M. Kardar, *Phys. Rev. Lett.* **106**, 210404 (2011).
- [19] R. Messina and M. Antezza, *Europhys. Lett.* **95**, 61002 (2011).
- [20] A. W. Rodriguez, O. Ilic, P. Bermel, I. Celanovic, J. D. Joannopoulos, M. Soljačić, and S. G. Johnson, *Phys. Rev. Lett.* **107**, 114302 (2011).
- [21] B.-S. Lu, D. S. Dean, and R. Podgornik, *Europhys. Lett.* **112**, 20001 (2015).
- [22] R. L. Jaffe, *Phys. Rev. D* **72**, 021301(R) (2005).
- [23] J. Cugnon, *Few-Body Syst.* **53**, 181 (2012).
- [24] Y. Levin, *Physica (Amsterdam)* **265A**, 432 (1999).
- [25] P. R. Buenzli and Ph. A. Martin, *Europhys. Lett.* **72**, 42 (2005).
- [26] B. Jancovici and L. Samaj, *Europhys. Lett.* **72**, 35 (2005).
- [27] If the circuit of plate 2 is closed, a current is induced in the plate 2 by the *Coulomb drag* due to plate 1; this is the case considered here. If the circuit of the opposing plate is open, charge accumulates at the plate edges, creating an in-plane electrical field which cancels due to the driven plate and prevents current flow in the opposing plate. This open configuration can be studied both numerically and analytically and is left for further study.
- [28] D. S. Dean and R. Podgornik, *Phys. Rev. E* **89**, 032117 (2014).
- [29] An electric current in one plate will lead to a steady state where this plate will have a higher temperature than the other. A difference in temperature can be taken into account in both our numerical and analytic treatment [21] of the problem; however, for the sake of simplicity it is not studied in this Letter.
- [30] See Supplemental Material at <http://link.aps.org/supplemental/10.1103/PhysRevLett.116.240602> for details of the numerical calculations and as well as details of the analytic derivation of the normal and lateral forces, which includes Refs. [31–34].
- [31] H. Flyvbjerg and H. G. Petersen, *J. Chem. Phys.* **91**, 461 (1989).
- [32] A. S. Kronfeld, *Prog. Theor. Phys.* **111**, 293 (1993).
- [33] E. Wigner, *Phys. Rev.* **40**, 749 (1932).
- [34] J. J. Weis, D. Levesque, and J. M. Caillol, *J. Chem. Phys.* **109**, 7486 (1998).
- [35] I.-C. Yeh and M. L. Berkowitz, *J. Chem. Phys.* **111**, 3155 (1999).
- [36] D. S. Dean, *J. Phys. A* **29**, L613 (1996).
- [37] K. Kawasaki, *Physica A (Amsterdam)* **208A**, 35 (1994).
- [38] *The Collected Works of Lars Onsager (with commentary)*, edited by P. C. Hemmer, H. Holden, and S. Kjelstrup Ratkje (World Scientific, Singapore, 1996).
- [39] V. Démery and D. S. Dean, *J. Stat. Mech.* (2016) P023106.
- [40] R. Zwanzig, *Non Equilibrium Statistical Mechanics* (Oxford University Press, Oxford, 2001).
- [41] V. Démery and D. S. Dean, *Phys. Rev. Lett.* **104**, 080601 (2010).
- [42] V. Démery and D. S. Dean, *Phys. Rev. E* **84**, 010103(R) (2011).